Compact actuation through magnetorheological flow control and rectification of magnetostrictive vibrations

David T. Nosse[a] and Marcelo J. Dapino[a]

[a]Department of Mechanical Engineering, The Ohio State University, Columbus, OH 43202

ABSTRACT

There is currently a need for compact actuators capable of producing large deflections, large forces, and broad frequency bandwidth. In all existing active materials, large force and broadband responses are obtained at small displacements and methods for transmitting very short transducer element motion to large deformations need to be developed. This paper addresses the development of a hybrid actuator which provides virtually unlimited deflections and large forces through magnetorheological (MR) flow control and rectification of the resonant mechanical vibrations produced by a magnetostrictive Terfenol-D pump. The device is a compact, self-contained unit which is capable of producing large work output. To achieve large output force, hydraulic advantage is created by implementing a driven piston diameter that is larger than the drive piston. Since the pump operates at high speeds, a fast-acting MR fluid valve is required. The paper presents a four-port MR fluid valve in which the fluid controls its own flow while carrying the full actuator load. A multi-domain model of the device was developed with the primary goal of analyzing and demonstrating the MR fluid valve concept. A research valve was designed, constructed, and tested for purposes of model parameter identification and validation, and analysis of device behavior. Deflections of over 6 in are demonstrated with the device presented here.

Keywords: Hybrid actuator, rectification valve, magnetorheological (MR) fluids, magnetostrictive pump, Terfenol-D, magnetorheological fluid valve, hydraulic advantage

1. INTRODUCTION

Many novel smart material actuator concepts have been studied and developed in recent years for use in a wide range of applications where high power density and broad frequency bandwidth actuation is required. Applications which can benefit from new actuator technologies include, among others, compact haptic interfaces, control surfaces for unmanned vehicles, actuator-based active suspension systems for heavy-duty commercial vehicles, adaptive airframes and rotors, and robotic locomotion components.

Some of the smart material transduction technologies being investigated can in certain cases exceed the power density of conventional electromagnetic devices, as is the case for example with the nickel titanium alloys. In these alloys, however, large displacements are obtained at the expense of small forces or slow frequency responses. Materials with faster reaction times, such as magnetostrictive or piezoelectric materials, have insufficient energy densities so use of these materials is typically restricted to low-displacement, high-force applications. Novel methods for converting very short deformation into large motion must therefore be developed.

Piezoelectric stack actuators have been used in hydraulic fluid pumps,[1–3] inchworm devices,[4] and kinematic linkages[5] for the purpose of large linear motion. Although commercially available piezoelectric stack actuators are capable of generating strains of 0.10 – 0.15% (1,000 – 1,500 $\mu\epsilon$) and potentially larger deformations via motion amplification mechanisms, the operating frequency and amplitude of these deformations are limited by dielectric losses and self-heating during dynamic operation. Normal low voltage actuators with mid sized diameters tend to overheat at frequencies in the range of about 200 Hertz at full stroke operation, which severely limits the rate of actuation. Sirohi and Chopra[1] were able to increase the frequency of steady state operation of a piezoelectric pump to 1000 Hz by using a thermally conducting silicone heat sink, but they accomplished so at the expense of overall system efficiency.

The most advanced giant magnetostrictive materials produce static strains on the order of 1,600 $\mu\epsilon$ at fields of 150 kA/m and loads of less than 14 MPa. Methods considered for amplifying these deformations include

Send correspondence to M.J.D.: Email: dapino.1@osu.edu Ph.: (614)-688-3689 Fax: (614) 292-3163

Smart Structures and Materials 2005: Smart Structures and Integrated Systems, edited by Alison B. Flatau, Proc. of SPIE Vol. 5764 (SPIE, Bellingham, WA, 2005)
0277-786X/05/$15 · doi: 10.1117/12.605444

mechanical amplifiers[6] and inchworm concepts.[7] These methods, however, have some intrinsic problems such as wear and backlash and are thus unsuitable for applications which require maintenance-free operation or which are life-critical.

Magnetorheological fluids undergo an apparent increase in viscosity within milliseconds of being exposed to a magnetic field.[11] While MR fluids are being increasingly used commercially in automotive and seismic dampers,[12,13] novel actuator concepts based on these fluids are scarce.[14,15] This paper implements the controllable rheological behavior of MR fluid coupled with the giant magnetostrain of a Terfenol-D MR fluid pump in a new hybrid actuator design. The combination of giant magnetostrain and robust operation make Terfenol-D particularly well suited for driving a piston-type fluid pump.[8–10] The power density of the proposed actuator is expected to be on the same range as that of pneumatic or low-range hydraulic actuators. The self-contained design of our actuator precludes the use of bulky external support components necessary for pneumatic and hydraulic actuator operation (i.e. supply lines, compressors). In addition, our concept circumvents the parasitic wear and backlash problems common to hydraulics.

The principle of operation of the actuator is presented in Sec. 2, followed by a discussion of the experiments in Sec. 3. The model is presented in Sec.4 and a discussion of model results is presented in Sec. 5. Finally, the concluding remarks are presented in Sec. 6.

2. HYBRID ACTUATOR PRINCIPLE OF OPERATION

The hybrid actuator design presented in this paper can produce large linear displacements and forces by the integration of Terfenol-D and magnetorheological fluid. The principle for achieving compact actuation is based on two effects: (i) rectification of resonant vibration produced by a magnetostrictive Terfenol-D pump through MR fluid flow control and (ii) utilization of hydraulic advantage for conversion of magnetostrain into large deflection and force. The main components of the hybrid magnetostrictive-magnetorheological actuator are shown in Fig. 1(a)-(c). The system consists of a four-port MR fluid valve, MR fluid, Terfenol-D pump, drive piston, and driven piston. To achieve rectification of the resonant vibrations produced by the Terfenol-D pump, and thus large deflections, the actuator operates through cyclic repetition of two stages, actuator extension and fluid refill. At each stage the MR fluid valve completely closes one half of the fluid circuit and permits free flow through the other.

Flow generated by the Terfenol-D pump and driving piston is routed through two parallel flow paths, that is with common pressure differential. Each fluid route includes one half of the MR fluid valve, and one path includes a driven piston to translate the flow to linear actuation. The MR fluid valve has two conical ends, each fitted with a permanent magnet. Solenoids wrapped around the valve at each end are used to cancel the field produced by the permanent magnets. When the solenoid around the valve has no applied current, there is no magnetic field cancelation and the MR fluid increases in viscosity. When a suitable current is applied, the coil's magnetic field cancels the permanent magnet's field and the MR fluid decreases in viscosity, thus permitting flow through the valve. This design creates a normally-on mechanism that locks the actuator in place in the event of power failure.

The actuator extension stage commences with the leftmost solenoid turned on and the rightmost turned off, as shown in Fig. 1(b). This effectively thickens the MR fluid in the right path, producing a fluid path of least resistance through the left valve half. The flow produced by the Terfenol-D pump produces a pressure differential that fully closes the right valve half with the assistance of the MR fluid, which when energized by magnetic fields behaves as an o-ring around the conical head. Once the right valve half has closed, the flow extends the driven piston for positive actuation. To increase the output force, a hydraulic advantage is created by implementing a driven piston diameter that is larger than the drive piston.

The fluid refill stage immediately follows as the Terfenol-D element and drive piston begin to retract, as shown in Fig. 1(c). To refill the fluid cavity without also retracting the actuator output, the left solenoid is turned off and the right turned on. This changes the fluid path of least resistance and creates the pressure differential necessary to begin closing of the leftmost valve half. With the left half closed, the actuator output is temporarily locked, and the free flow path through the opened right valve refills the cavity. Steps (b) and (c) are subsequently repeated at high speed to further extend the driven piston and thus achieve quasi continuous motion of the load attached to the actuator.

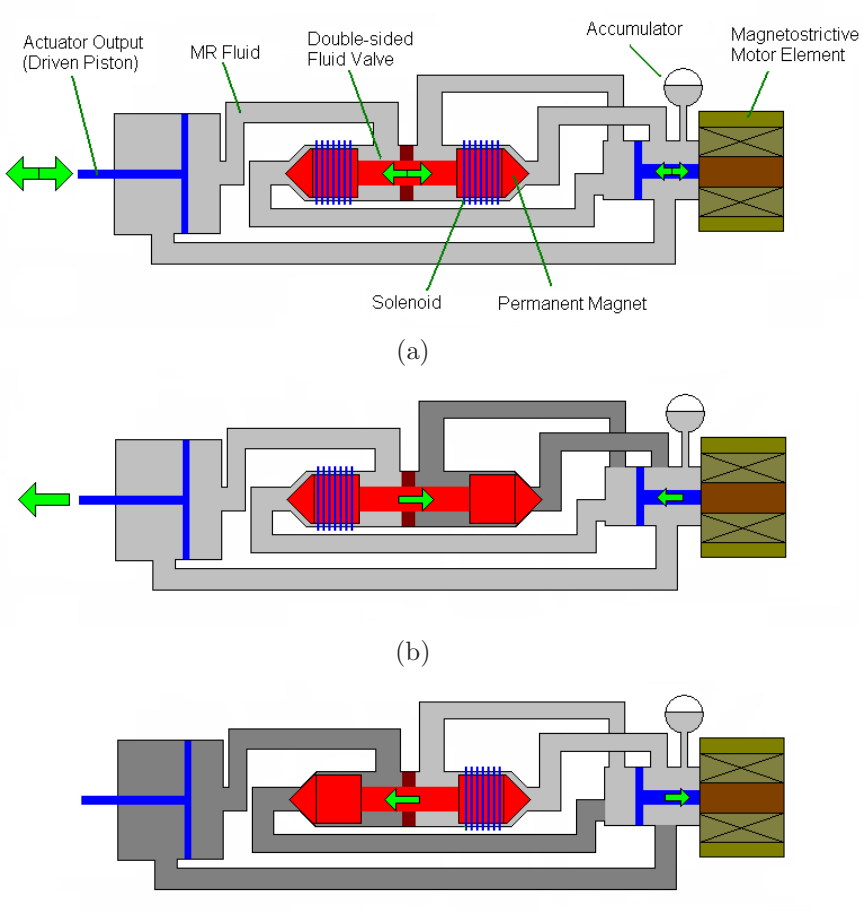

Figure 1. (a) Hybrid MR fluid-magnetostrictive actuator. In (b), the drive piston connected to the Terfenol-D pump pushes the fluid through the left valve half and subsequently pushes the driven piston on the load end (left coil active), while the right valve half remains closed. In (c), the drive piston retracts while the MR fluid recirculates through the right half valve (right coil active). The driven piston stays fixed until step (b) starts again and the sequence is repeated. Permanent magnets inside the conical heads provide a bias force on the MR fluid.

3. EXPERIMENTS

3.1. Constructive Details

An actuator was developed to identify model parameters and analyze the behavior of the device. The experimental setup is shown in Fig. 2(a)–(b) and consists of a four-port, two-sided magnetorheological fluid valve, input and output hydraulic pistons, and steel lines to complete the closed MR fluid network.

The MR fluid valve, shown in Fig. 3, consists of two conical heads, each embedded with two solenoids and no permanent magnets. Using this design, power must be applied to the fluid valve for it to close to one side making it a "normally open" valve. This oversized design is easier to implement and offers greater magnetic field adjustability, thus it is preferable from a development point of view. Due to the oversized valve design, the Terfenol-D pump is unable to produce the necessary fluid input quantities for fluid pressure and volume flow rate. The fluid inputs are temporarily generated by a double-ended hydraulic piston connected to a universal compression-tension machine until further valve miniaturization is implemented.

The hydraulic fittings and connectors of closed fluid network were strategically placed to aid in both fluid filling and air removal. Components were filled both individually before being connected to the system and

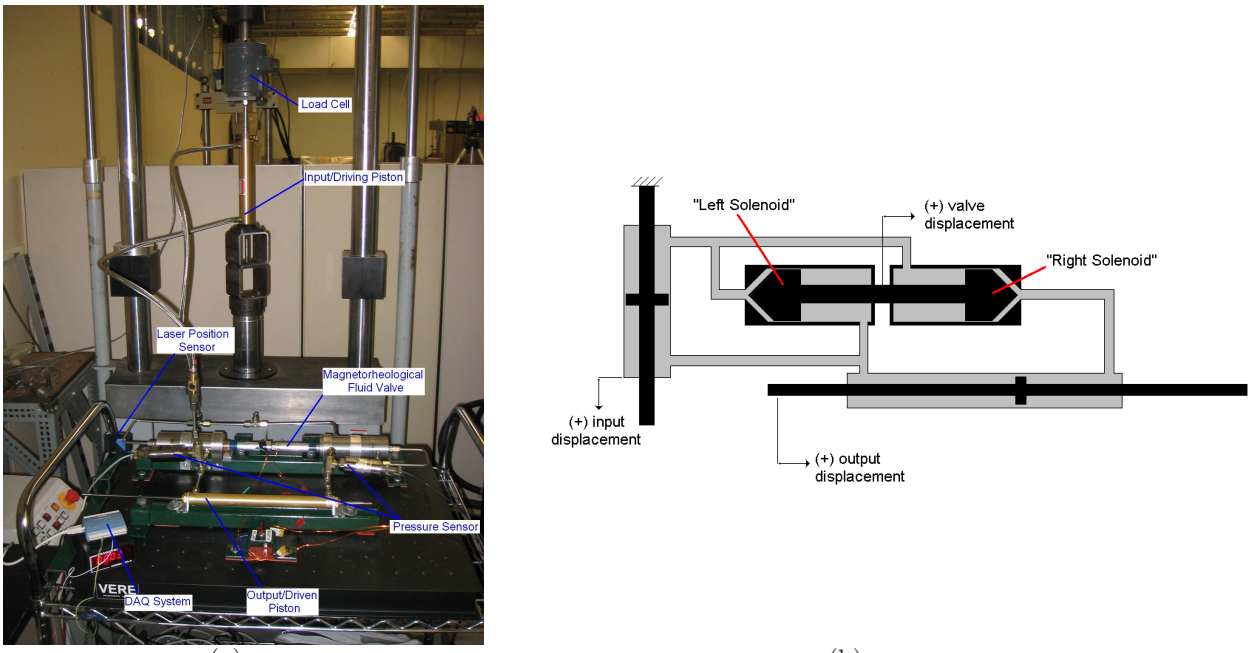

(a) (b)

Figure 2. (a) Experimental setup used for development and testing of the MR fluid valve and hybrid actuator. (b) Illustration of setup, definition of "left" and "right" solenoids, and direction reference.

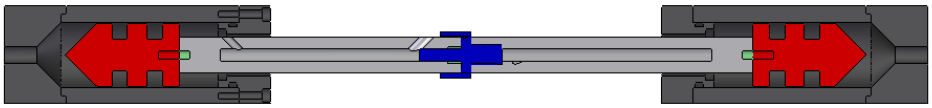

Figure 3. Cutaway solid model of the MR fluid valve. The grooves in the conical valve ends are fitted with coils for enhanced flexibility compared with the final design which employs permanent magnets.

after being fastened tight to reduce the amount of trapped air. When applicable, hard steel lines were used to connect fluid components while minimizing capacitance. All hard steel lines were bent at angles no tighter than 90 degrees and arranged so that all lines were on the same horizontal plane to reduce unwanted fluid resistance asymmetries. Two braided steel lines were needed to permit relative motion between the input piston and the remaining components. It is noted that all fluid lines will be internally incorporated in the final actuator design. For both the input and output hydraulic cylinders, the pistons have double-ended rods to provide a constant internal volume. Single-ended piston rods would produce unwanted fluid vacuums, cavitation and variable pressure biases dependent on the positions of both pistons.

A LabVIEW VI (Virtual Instrument) was developed for recording data on two data acquisition instruments from the following five sources: universal compression-tension machine applied load or position, two fluid line pressure sensors, MR fluid valve position, and output piston position. The LabVIEW program is also capable of producing an output voltage to control the magnetic fields based on a prescribed control algorithm.

3.2. Valve Resistance Measurements

The ability of the MR fluid valve to control the fluid flow was experimentally tested by temporarily isolating components of the system. The main fluid resistance parameters were identified to be valve position, magnetic field applied to the MR fluid, and flow direction. Individually, each valve half was connected to the input piston as shown in Fig. 4(a). A valve position locking mechanism was constructed to hold a constant gap for the entire duration of a run, with the gap as defined in Fig. 4(b). Maintaining a fixed gap is necessary to isolate the

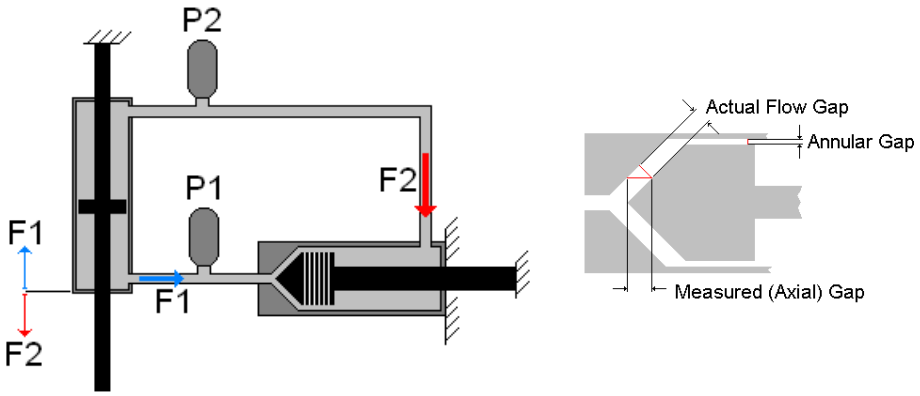

(a) (b)

Figure 4. (a) Illustration of the setup used to determine valve resistance. The arrows indicate the two flow directions, F1 and F2, relative to the input provided by the compression machine. (b) Gap definitions.

parameter of valve location from the resistance measurements. The coil voltage was kept constant throughout each run by a DC power source and amplifier. From the measured pressures $P1$ and $P2$, the fluid resistance R was characterized by

$$R = \frac{P_2 - P_1}{Q_v}, \tag{1}$$

where Q_v is the volume flow rate. To remove unwanted dynamic effects from the measurement, a triangular waveform (0.25 Hz, 4 in pk–pk) was selected as the input piston (fluid volume) displacement, as seen in Fig. 5(a). Triangular waves have constant derivatives (Q_v) between peaks, which allows for constant flow rate measurements to be made as shown in Fig. 5(b). The four-second period is sufficiently long to remove dynamic effects but short enough to produce sufficiently large pressures. It is noted that although equal flow rate waveforms were input for all resistance tests, the force applied by the compression machine varies significantly from run to run, as it is dependent on the resistance of the fluid path.

To illustrate, Fig. 5(c) shows the line pressures for the left valve, 10 V input, and 0.125 in axial gap run, whereas the calculated resistance corresponding to the same run is shown in Fig. 5(d). It is noted that for both shear and flow modes, the gap perpendicular to the flow direction is of primary interest. The test variables include two different annular gaps (0.030 and 0.125 inches), three dc drive voltages applied to the solenoid (0, 5 and 10 volts), up to five axial gaps (0.036, 0.057, 0.075, 0.125 and 0.250 inches), and two flow directions (F1 and F2). For best valve operation, it is desired to achieve the highest resistance possible at full voltage and the lowest resistance possible at no voltage. The resistance values are practically the same regardless of the flow direction. The varying fluid resistances based on position and magnetic field for two annular gaps (0.030 in and 0.125 in) were tested and are summarized in Fig. 6. The valve with an annular ring gap of 0.125 in is able to increase the MR fluid viscosity such that the resistance with an applied magnetic field approximately doubles the no field resistance. However, the valve with 0.030 in annular gap is effectively able to increase resistance by a factor of between four to five. Therefore, the annular gap dimension of the MR fluid valve required to effectively control its own flow is approximately 0.030 in.

3.3. Controlled Actuation

The ability of the MR fluid valve to produce sufficient pressures to extend a hydraulic output piston was tested using the setup shown in Fig. 2(a). From the resistance measurements discussed in Sec. 3.2, the 0.030 in annular gap dimension was selected for the MR fluid valve for its increased flow control ability. In terms of frequency response, the relatively large quantity of fluid within the closed fluid network significantly reduces the bandwidth of the actuator presented here relative to the final, miniaturized device. The optimum operating range of the

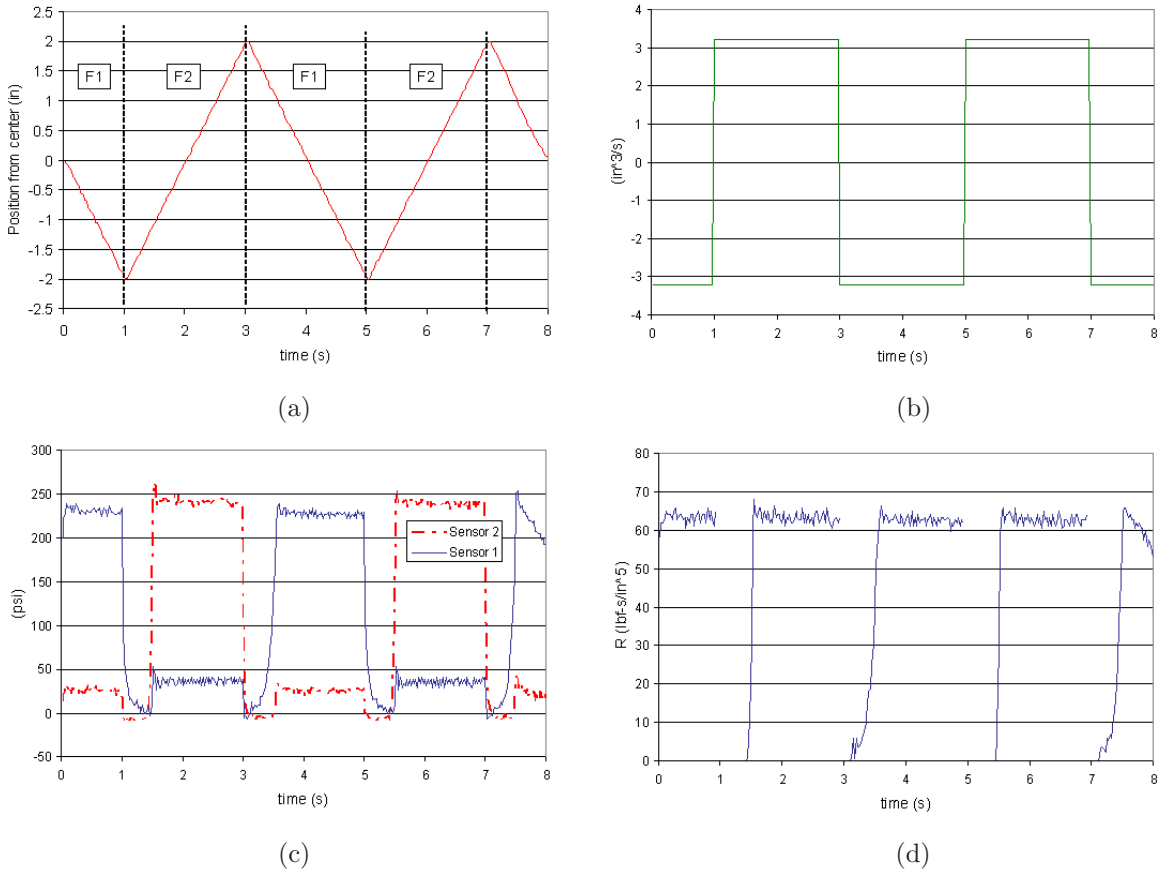

Figure 5. Data for left valve half, 10 V dc excitation, 0.125 in axial gap, 0.030 in annular gap. (a) Input piston position, (b) input flow rate, (c) line pressures, and (d) resistance.

Annular Gap (in)	Voltage (V)	Axial Gap (in)	Avg. Resistance (lbf*s/in^5)	
			Flow Direction: F1	Flow Direction: F2
0.03	0	0.250	11	12
		0.125	11	12
		0.075	12	12
		0.057	16	17
		0.036	20	20
	5	0.250	49	50
		0.125	52	53
		0.075	45	46
		0.057	72	74
		0.036	84	91
	10	0.250	56	58
		0.125	60	60
		0.075	52	53
		0.057	80	82
		0.036	93	100
0.125	0	0.250	9	9
		0.125	9	9
		0.075	9	10
	5	0.250	16	17
		0.125	18	18
		0.075	21	22
	10	0.250	19	19
		0.125	20	21
		0.075	19	19

Figure 6. Valve resistance measurements for two different annular gaps, three drive voltages applied to the solenoid, up to five axial gaps, and two flow directions.

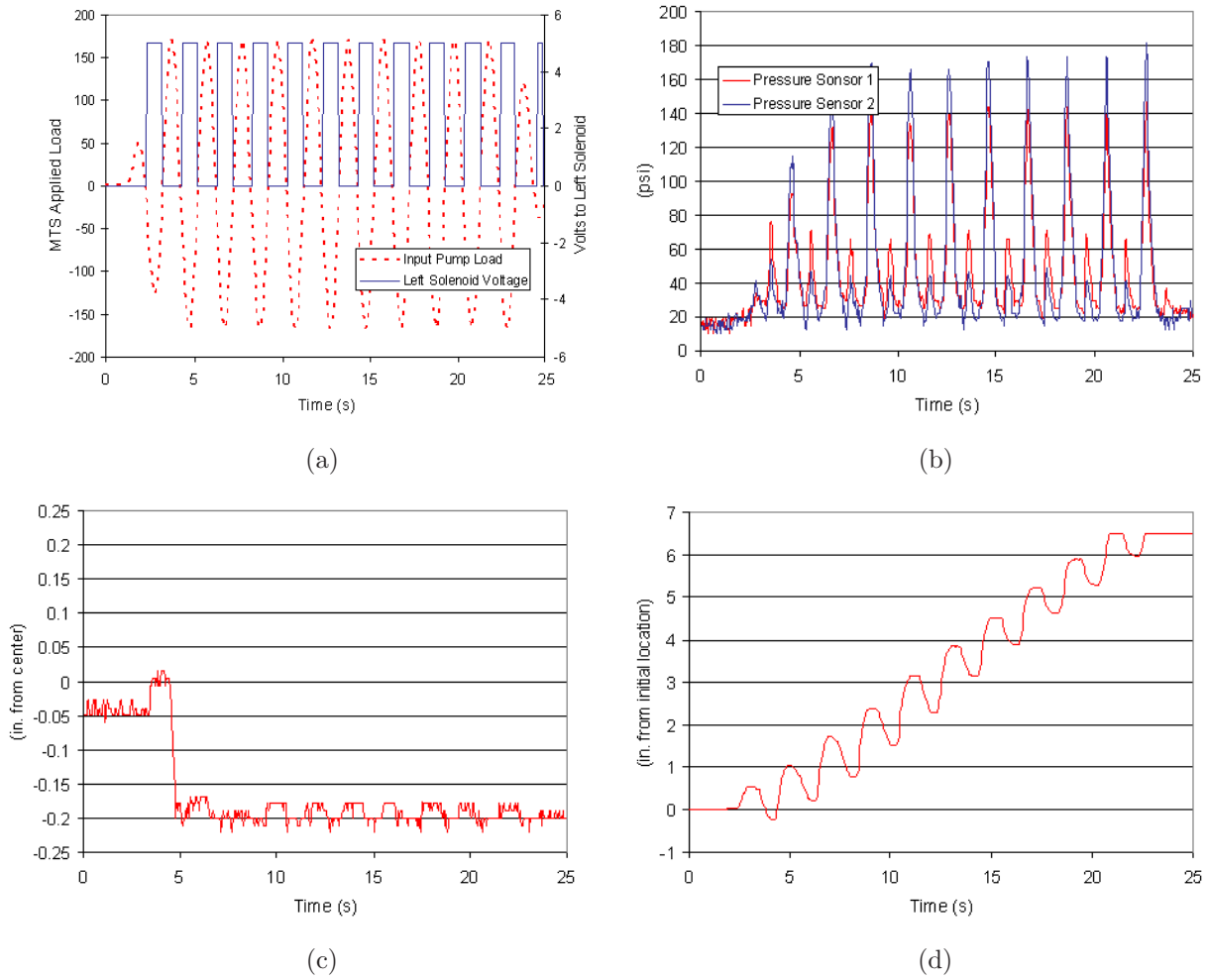

Figure 7. Actuation results (a) control strategy for 5 V dc solenoid input and negative (F1) input piston loading (b) line pressures (c) valve location, and (d) output piston position.

actuator was found to be between 0.25–0.75 Hz. Although the fluid inertia and resistance decrease with increasing line diameter, the fluid capacitance increases making the system softer. Thus, the smaller MR fluid valve and connecting lines in the final device will produce a much stiffer system capable of operating at higher frequencies.

The control strategy outlined in Section 2 involves applying square waves at a relative phase of 180 degrees between each solenoid. The measurements suggest that the removal of the voltage to the right valve half (in series with the output piston) has little effect on the output actuation. This is attributed to the unequal resistances when "unpowered" caused by one path having the output hydraulic piston. Thus, for all controlled actuation data presented, no voltages were applied to the right valve half.

A net actuation of 6.5 in was achieved at a rate of 0.325 in/s from a 1.0 in, 0.5 Hz sine wave driving piston input and 5 V square wave applied during negative (F1) input piston loading. The recorded results are presented in Fig. 7. The output actuation motion shown in Fig. 7(d) is a ramped sinusoid. Further design modifications are necessary to reduce the amount of motion reversal, and thus increase the net positive actuation and system efficiency. Another significant departure from the valve concept presented in Section 2 is that the MR fluid valve does not close completely one half, then completely close the other valve half. Instead, it quickly moves toward the controlled solenoid side (side not in series with output piston) and fluctuates small amounts from completely closed to slightly open. This is attributed mainly to large sliding frictions observed in the valve.

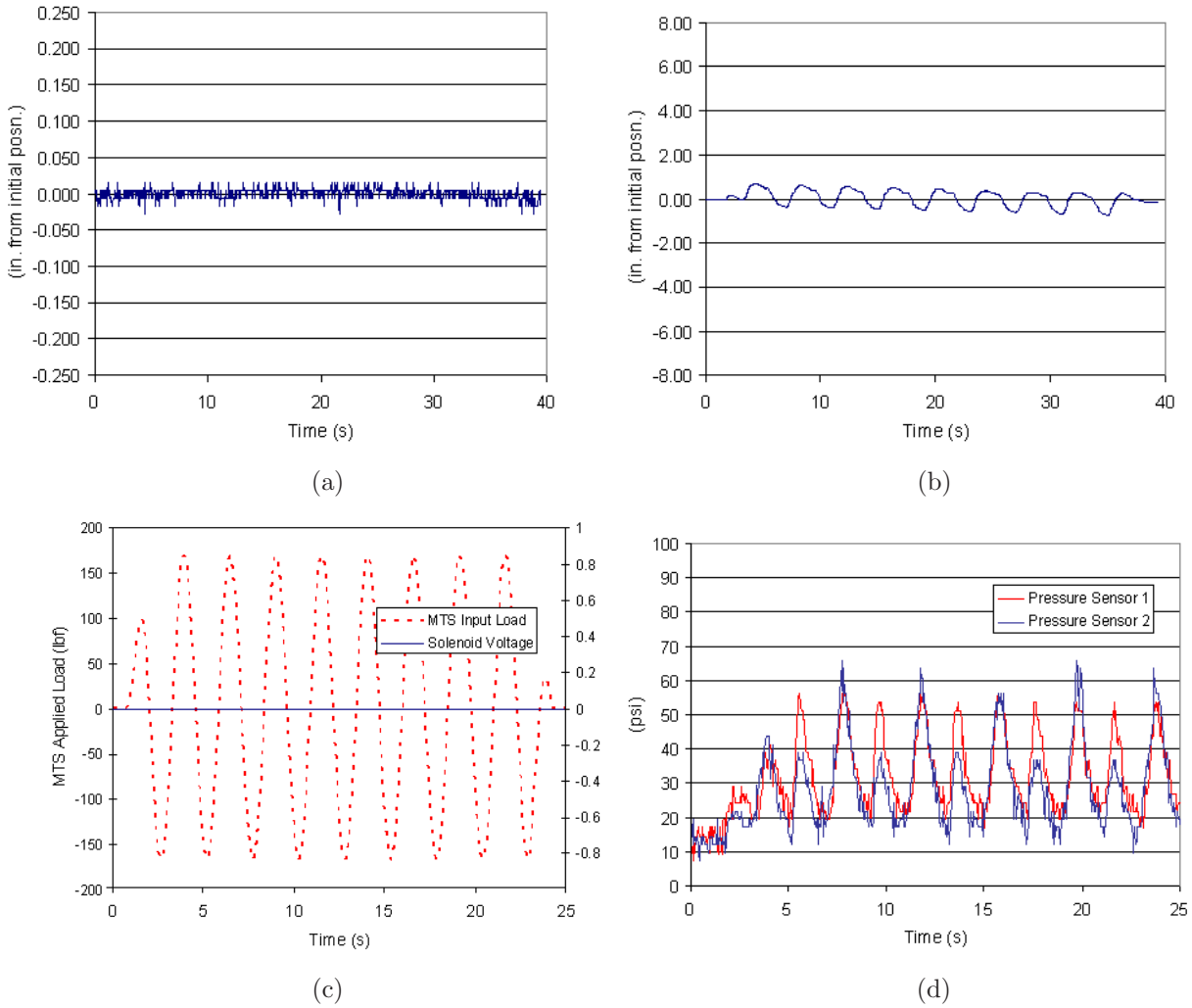

Figure 8. Actuation results (a) control strategy for 5 V dc solenoid input and negative (F1) input piston loading, (b) line pressures, (c) valve location (-0.2 in is valve not in series with output piston closed), and (d) output piston position.

To verify the need for MR fluid and its ability to increase in viscosity, as opposed to using ordinary hydraulic oil, a similar experiment was run with the no voltage input to the solenoids. The results presented in Fig. 8 show minimal actuation and valve motion. The fluid pressures and shear stresses cannot control the valve and output piston. Therefore, MR fluid is required as the working hydraulic fluid.

4. SYSTEMS MODEL

In conjunction with experimental testing, a system model of the hybrid actuator was developed and programmed in Simulink. A robust model will further verify the concept, but also aid in the redesign of the oversized concept actuator. The presented model is the second iteration. The first iteration was a multi-physics domain model where energy was converted from electrical, fluid, and mechanical domains via coupling equations. However, the model construction mandated the use of unideal system inputs, which rendered the simulations unnecessarily cumbersome and complex. Furthermore, highly nonlinear terms made the model unstable.

The presented model primarily uses fluid equations and experimental data look-up tables to calculate system outputs. The system is described by Fig. 9. Controlled inputs to the model are ON/OFF saturation voltages for the left V_L and right V_R solenoid, acceleration $\ddot{x}$ of the input hydraulic piston, and the force F_1 required to

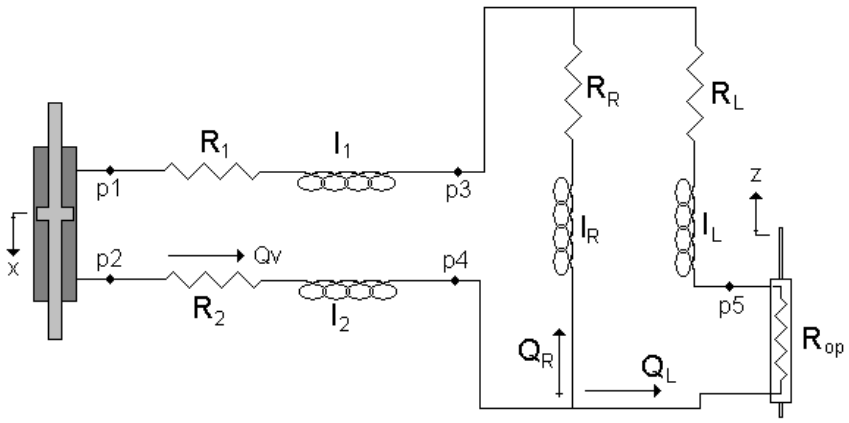

Figure 9. System level representation of the hybrid actuator, in which the fluid flow is represented by resistance and inductance elements.

accelerate the input piston of mass M. The following set of equations provides a solution for the input pressure differential p_2 - p_1 by means of Newton's Law, force balancing, flow resistance, and volume flow rate Q_v.

$$\sum F = M\frac{d^2x}{dt^2} \tag{2}$$

$$F_1 + p_1A_{ip} - p_2A_{ip} = M\frac{d^2x}{dt^2} \tag{3}$$

$$p_2 - p1 = \frac{F_1 - M\ddot{x}}{A_{ip}} \tag{4}$$

$$Q_v = \frac{dx}{dt}A_{ip} \tag{5}$$

Here, A_{ip} is the input piston cross sectional area. Pressure losses occur between the input piston and the valve from flow within the fluid lines. Assuming negligible fluid capacitance due to the stiff lines and incompressible fluid, then all pressure loss occurs from resistance and inertia effects. Since R_1 and I_1 are approximately equal to R_2 and I_2, both variables are set equal as R and I. Assigning a constant fluid resistance to the output piston R_{op}, the pressure differentials are

$$p_4 - p_3 = p_2 - p_1 + 2(RQ_v + I\frac{dQ_v}{dt}), \tag{6}$$

$$p_4 - p_3 = R_LQ_L + I_L\frac{dQ_L}{dt}, \tag{7}$$

$$p_5 - p_3 = R_RQ_R + I_R\frac{dQ_R}{dt}, \tag{8}$$

$$p_4 - p_5 = R_{op}Q_R, \tag{9}$$

$$p_4 - p_3 = R_RQ_R + I_R\frac{dQ_R}{dt} + R_{op}Q_R. \tag{10}$$

The fluid parameters are estimated by[16]

$$R_1 = \frac{128\mu L}{\pi d^4}, \tag{11}$$

$$I_1 = 2\left(\frac{\rho}{A}\right)L. \tag{12}$$

The total flow volume divides into two fluid paths connected in parallel while observing conservation of mass laws (13) and (14). Q_R is the volume flow rate of MR fluid through the right valve half and output piston, and Q_L is the volume flow rate through the left valve half. This permits calculation of the volume flow rates through each valve half, as a function of the variable valve-half resistances by setting equations (7) and (10) equal and solving (13) and (14) for Q_R and $\frac{dQ_L}{dt}$. The resultant flow divider equation is (15).

$$Q_v = Q_R + Q_L, \tag{13}$$

$$\frac{dQ_v}{dt} = \frac{dQ_R}{dt} + \frac{dQ_L}{dt}, \tag{14}$$

$$(R_r + R_{op} + R_L)Q_R + (I_R + I_L)\frac{dQ_R}{dt} = (R_R + R_{op})Q_v + I_R\frac{dQ_v}{dt}. \tag{15}$$

The fluid leakage across each valve half is a function of the variable valve resistances, which are dependent on valve position y, flow direction, and input voltages V_L and V_R, and the divided volume flow rates. The experimental values obtained from Section 3.2 are implemented in a look-up table within the simulation to model the leakage output based on resistance and pressure differential inputs. The stored fluid within each valve housing is thus able to control the position of the fluid valve y.

The position of the output piston z and actuation force F_z are modeled by the following equations, where A_{op} is the output piston cross sectional area.

$$V_R = \int Q_R, \tag{16}$$

$$z = \frac{V_R}{A_{op}}, \tag{17}$$

$$F_z = \frac{p_4 - p_5}{A_{op}}. \tag{18}$$

$$\tag{19}$$

5. MODEL RESULTS AND DISCUSSION

The actuator model is compared to the experimental results presented in Fig. 7. Analogous inputs for each run were used, which includes a 0.5 Hz 1 in amplitude sinusoidal input piston position waveform, a 0.5 Hz, 100 lbf amplitude sinusoidal input piston force waveform, and a 5 V left solenoid control voltage (square waveform). The model output is shown in Fig. 10. Several performance characteristics observed experimentally are captured by the model. The valve position y starts at the midpoint and quickly biases itself towards the left closed location (-0.20 in = left valve half closed, +0.20 in = right valve half closed). Throughout the entire run, the valve cycles between fully closed and being slightly open. The model's output piston position z has the shape of a ramped sinusoid, consistent with the experiments. However, the model's actuation rate of 1.5 in/s, is approximately 4.6 times greater than the measured actuation. This difference is attributed mainly to the sliding friction between the valve housing and movable shaft not being incorporated into the current model. Thus, minimizing sliding friction in future MR fluid valve designs should increase actuator performance.

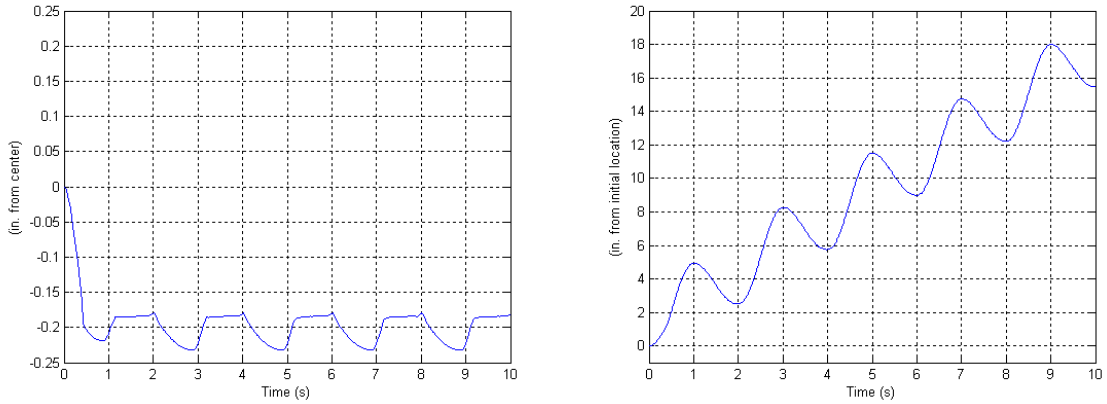

(a) (b)

Figure 10. Model results for (a) valve location (-0.20 in = left valve half closed, +0.20 in = right valve half closed) and (b) output piston location.

6. CONCLUDING REMARKS

In various industry sectors, both traditional and emerging, there is a need for compact, high-power, and broadband actuators. The actuator design presented in this paper is a hybrid of two smart materials, magnetorheological (MR) fluid and Terfenol-D. A prototype double-sided, four-port MR fluid valve was fabricated and tested. Among the tested properties was the variable fluid resistance as a function of voltage, position, and flow direction. The data were collected for use in a system model developed in Simulink. A research actuator was constructed using the MR fluid valve and a universal compression-tension machine as a temporary substitution for the Terfenol-D pump. Experimental results verified that positive actuation is possible with proper solenoid input timing and that MR fluid is indeed needed to rectify the input motion to a usable linear output. The model confirmed the experimental findings that the hybrid actuator concept is capable of producing large deformations of over 6 in.

7. ACKNOWLEDGMENTS

This work was supported by the Defense Advanced Research Projects Agency (DARPA) (John Main program manager) through Air Force Research Laboratory, Space Vehicle Directorate grant FA9453-03-C-0333 (Scott Franke program monitor). The authors wish to acknowledge William Gillespie and Scott Stacey at Delphi Chassis & Energy for supplying the MR fluid used in this investigation.

REFERENCES

1. J. Sirohi and I. Chopra, "Design and development of a high pumping frequency piezoelectric-hydraulic hybrid actuator," *Journal of Intelligent Material Systems and Structures* **14**, pp. 135–147, 2003.
2. L. D. Mauck and C. S. Lynch, "Piezoelectric hydraulic pump development," *Journal of Intelligent Material Systems and Structures* **11**, pp. 758–764, 2000.
3. D. G. Lee, S. Wing, and G. P. Carman, "Design of a piezoelectric-hydraulic pump with active valves," *Journal of Intelligent Material Systems and Structures* **15**, pp. 107–115, 2004.
4. J. Park, G. P. Carman, and H. T. Hahn, "Design and testing of a mesoscale piezoelectric inchworm actuator with microridges," *Journal of Intelligent Material Systems and Structures* **11**, pp. 671–684, 2000.
5. E. F. Prechtl and S. R. Hall, "Design of high efficiency, large stroke, electromechanical actuator," *Smart Materials and Structures* **8**, pp. 13–30, 1999.
6. S. Canfield and M. Frecker, "Topology optimization of compliant mechanical amplifiers for piezoelectric actuators," *Structural and Multidisciplinary Optimization* **20**, pp. 269–279, 2000.
7. L. P. Davis, ed., "Terfenol-D in linear motors," *Proc. 2nd Inter. Conf. Giant Magnetostrictive Alloys*, 1998.

8. K. Bridger, J. M. Sewell, A. V. Cooke, J. L. Lutian, D. Kohlhafer, G. E. Small, and P. M. Kuhn, "High-pressure magnetostrictive pump development: a comparison of prototype and modeled performance," in *Smart Structures and Materials 2004: Industrial and Commercial Applications of Smart Structures Technologies*, E. H. Anderson, ed., *Proc. SPIE* **5388**, pp. 246–257, 2004.
9. J. P. Teter, M. H. Sendaula, J. Vranish, and E. J. Crawford, "Magnetostrictive linear motor development," *IEEE Transactions on Magnetics* **34**, pp. 2081–2083, 1998.
10. N. Lhermet, F. Claeyssen and H. Fabbro, "Electro-fluidic components based on smart materials for aircraft electro-hydraulic actuators," *9th Inter. Conf. New Actuators*, 2004.
11. M. R. Jolly, J. W. Bender, and J. D. Carlson, "Properties and applications of commercial magnetorheological fluids," in *Smart Structures and Materials 1998: Passive Damping and Isolation*, L. P. Davis, ed., *Proc. SPIE* **3327**, pp. 262–275, 1998.
12. H. J. Jung, B. F. S. Jr, Y. Q. Ni, and I. W. Lee, "State-of-the-art of semiactive control systems using mr fluid dampers in civil engineering applications," *Structural Engineering and Mechanics* , 2002.
13. Y-T. Choi and N. M. Wereley, "Quasi-steady analysis of a magnetorheological dashpot damper," *Proc. IMECE'04*, 2004.
14. J. H. Yoo, J. Sirohi, N. M. Wereley and I. Chopra, "A Magnetorheological Hydraulic Actuator Driven by a Piezopump," *Proc. IMECE'03*, 2003.
15. J.-H. Yoo and N. M. Wereley, "Performance of a magnetorheological hydraulic power actuation system," *Journal of Intelligent Material Systems and Structures* **15**, pp. 847–857, 2004.
16. J. L. Shearer, B. T. Kulakowski, and J. F. Gardner, *Dynamic modeling and control of engineering systems*, Prentice Hall (2nd Edition), 1997.